Flow in the driven cavity calculated by the lattice Boltzmann method

W. Miller
CRS4-Centre for Advanced Studies, Research and Developement, Via N. Sauro 10, I-90123 Cagliari, Italy
(Received 13 June 1994; revised manuscript received 19 September 1994)

The lattice Boltzmann method with enhanced collisions and rest particles is used to calculate the flow in a two-dimensional lid-driven cavity. The ability of this method to compute the velocity and the pressure of an incompressible fluid in a geometry with Dirichlet and Neumann boundary conditions is verified by calculating a test problem where the analytical solution is known. Different parameter configurations have been tested for Reynolds numbers from Re=10 to Re=2000. The vortex structure for a more generalized lid-driven cavity problem for different types of boundary conditions has been studied for three different aspect ratios.

PACS number(s): 02.70.Ns, 47.15.Rq, 47.20.Ft, 51.10.+y

I. INTRODUCTION

Lattice gas automata (LGA) are a rather new technique in the world of fluid mechanics, but since the first discovery of a LGA by Frisch, Hasslacher, and Pomeau [1], which reproduces all terms of the Navier-Stokes equations, they have undergone fast development. With the introduction of the lattice Boltzmann method (LBM) by McNamara and Zanetti [2] the statistical noise, present in the LGA, has been removed. Higuera, Succi, and Benzi developed the LBM with "enhanced collisions," where the foremost complicated collision operator was replaced by a much simpler one [3]. A further simplification can be achieved if the collision term is described by a simple relaxation. The LBM becomes then a Bhatnagar-Gross-Krook(BGK) model (Qian, D'Humières, and Lallemand [4]). The introduction of rest particles by Chen, Chen, and Matthaeus [5] removed the unphysical factor in the pressure term of the previous models and allowed the correct calculation of the pressure.

In this paper the LBM with enhanced collisions is extended by a reservoir of rest particles and used to study the flow and pressure distribution in a lid-driven cavity. There exists a particular benchmark problem introduced by Shih, Tan, and Hwang [6], where the analytical solution is known. This gives the possibility of testing the numerical code for both Dirichlet and Neumann boundary conditions and checking the influence of the parameters in the LBM on the result. Having verified that this method reproduces the analytic solution with small errors comparable to other numerical methods, I go beyond the theoretical solvable problem and study the flow in cavities of different aspect ratios driven by a uniform or nonuniform shear flow. Different vortex structures are observed for different kinds of boundary conditions, if the aspect ratio is 10.

II. THE LATTICE BOLTZMANN MODEL

In general a lattice gas automaton in D dimensions consists of particles moving on links ($i = 1, ..., M_{\vec{c}}$) of a lattice from one node $\vec{r}_*$ to the adjacent one, where they can collide with one another. The time evolution for the population n_i for particles with speed $\vec{c}_i$ is then given by a moving step and a collision, described by the operator Ω_{ij} (the time step is set equal to 1),

$$n_i(\vec{r}_* + \vec{c}_i, t_* + 1) = n_i(\vec{r}_*, t_*) + \Omega_{ij}. \tag{1}$$

Both operations conserve mass and momentum. Denoting the mean populations with $N_i(\vec{r}_*, t_*) \equiv \langle n_i(\vec{r}_*, t_*)\rangle$ the density ρ and velocity $\vec{u}$ are given by $\rho = \sum_i N_i$ and $\vec{u} = \frac{1}{\rho}\sum_i N_i \vec{c}_i$, respectively.

For the right choice of the lattice the model converges towards the Navier-Stokes equations in the continuum limit [1–7]. Assuming that all particles have the same speed, the equilibrium distribution for the population N_i is given in the small Mach number limit by

$$N_i^{eq} = d + \underbrace{d\frac{D}{c^2}(\vec{c}_i\vec{u})}_{N_i^{eq,1}} + \underbrace{d\frac{D(D+2)}{2c^4}g(\rho)[(\vec{c}_i\vec{u})^2 + h_2u^2]}_{N_i^{eq,2}} + O(u^3), \tag{2}$$

where

$$c = |\vec{c}_i|, \quad g(\rho) = \frac{D}{(D+2)}\frac{f''}{f'^2},$$

f is the distribution function of the lattice gas and f' and f'' its first and second derivatives at $|\vec{u}| = 0$, respectively. The expansion coefficient h_2 can be determined by the conservation of mass. Performing the continuum limit as a multiscale expansion in a small parameter ε

$$N_i = N_i^{eq} + \varepsilon N_i^{neq,1} + O(\varepsilon^2),$$

one arrives at the Navier-Stokes equations [1] with a pressure tensor,

$$\Pi_{\alpha\beta} = \underbrace{\rho c_s^2\left(1 - g(\rho)D\left[\frac{1}{2} + h_2\frac{D+2}{c^2}\right]\frac{u^2}{c^2}\right)}_{p}\delta_{\alpha\beta} + \rho g(\rho) u_\alpha u_\beta, \tag{3}$$

$c_s = \sqrt{(c^2/D)}$ is the sound speed and p the pressure. In the LBM the statistical avarages N_i are used in Eq. (1) instead of n_i and the collision operator is approximated by

$$\Omega_{ij} \approx \mathcal{A}_{ij}(N_j - N_j^{eq}). \tag{4}$$

If elements a_{ij} of the matrix $\mathcal{A}_{ij}$ depend only on the angle between i and j, they can be expressed by the leading eigenvalue λ of the matrix. In this LBM with *enhanced collisions* [3] is $-\frac{1}{\lambda}$ the relaxation time, in which the population N_i at a node converges to its equilibrium N_i^{eq} [8] and the viscosity ν is related to λ by the following relation:

$$\nu = -\frac{1}{3}\left(\frac{1}{\lambda} + \frac{1}{2}\right). \tag{5}$$

By introducing a reservoir of rest particles with a density d_0 the dependence of the pressure p on the velocity u can be removed [5]. The total density of the system is then given by

$$\rho = d_0 + M_{\vec{c}} d \tag{6}$$

with the density d of moving particles per node.

In the face-centered hypercubic (FCHC) lattice ($D = 4$, $M_{\vec{c}} = 24$, and $c = 2$) the equilibrium distributions can be written as

$$N_i^{eq} = d + \frac{\rho}{24}\left[2(c_i)_\alpha u_\alpha + 3(c_i)_\alpha (c_i)_\beta u_\alpha u_\beta - u^2\right] \tag{7}$$

for the moving particles and

$$N_0^{eq} = d_0 - \frac{\rho u^2}{2} \tag{8}$$

for the rest particles. The population of the particles N_0 relaxes into its equilibrium within the relaxation time of the system, i.e., within $\tau_{rel} = -\frac{1}{\lambda}$. Therefore, the time evolution of the population of rest particles is given by

$$N_0(\vec{r}_*, t_* + 1) = N_0(\vec{r}_*, t_*) + \lambda(N_0 - N_0^{eq}). \tag{9}$$

Because the rest particles are activated isotropically into moving particles, the time evolution of the populations of the moving particles has the following form:

$$N_i(\vec{r}_* + \vec{c}_i, t_* + 1) = N_i(\vec{r}_*, t_*) + \mathcal{A}_{ij}(N_j - N_j^{eq}) - \frac{\lambda}{24}(N_0 - N_0^{eq}). \tag{10}$$

In this paper I use a projection of the FCHC lattice on two dimensions which is described in detail in [8]. In total there are nine different populations for the moving particles, four in the axial directions ($i = 1, 3, 5, 7$) with $\vec{c}_i = \left(\cos\frac{i-1}{4}\pi, \sin\frac{i-1}{4}\pi\right)$ which have a weight of four due to the fact that each is the projection of four links from the original space, four in the diagonal direction ($i = 2, 4, 6, 8$) with $\vec{c}_i = \left(\cos\frac{i-1}{4}\pi, \sin\frac{i-1}{4}\pi\right)$, and one perpendicular to the plane, which has also a weight of four. The tenth population is that of rest particles. Therefore, the total density is given by $\rho = \sum_{i\,even} N_i + 4\sum_{i\,odd} N_i$.

The hydrodynamical system is described by the Reynolds number $\mathrm{Re} = \frac{l_0 u_0}{\nu}$ with the characteristic velocity u_0 and the number of mesh points l_0 for the characteristic length. The LBM used implies some restrictions on the velocity, where an upper limit of $u = 0.2$ (Mach number $M = 0.28$) has been found [9], and to the viscosity where a lower limit of $\nu = 0.14$ has been observed [9]. The upper limit for velocity results from the compressibility of the lattice gas used, because the spatial change of the density describes the pressure [see Eq. (3)]. If the velocity u becomes too large, the compressibility effect is not negligible any more. The lower limit for the viscosity has its origin in the relaxation behavior of the system, because $-\lambda = \frac{2}{6\nu+1}$ is the relaxation parameter ω and tends to two if the viscosity is decreased towards zero. If the overrelaxation ($\omega > 1$) is too large the system becomes unstable. The lower limit for ν mentioned above was derived from the numerical experience with the LBM without rest particles. The behavior of the LBM with rest particles is discussed in Sec. III.

From now on I change the notation in the following way: parameters in the LBM are labeled $_{LB}$ to distinguish them from the values in the "real world." I define $\hat{u}$ and $\hat{l}$ via

$$\vec{u} = \vec{u}_{LB}\hat{u} \qquad \text{and} \qquad l = l_{LB}\hat{l}, \tag{11}$$

respectively. If the normalized pressure $p = \frac{p'}{\rho}$ is used, where p' is pressure and ρ the density, the normalized pressure can be obtained from the variation $\delta\rho_{LB}$ in the mean density $\overline{\rho_{LB}}$ via

$$p = \frac{\delta\rho_{LB}}{\overline{\rho_{LB}}}\frac{\hat{u}^2}{2}. \tag{12}$$

The relation for a body force $\vec{f}$ is

$$\vec{f} = \frac{\hat{l}}{\hat{u}^2}\vec{f}_{LB}. \tag{13}$$

In the following I will give a short description of how I implement the boundary conditions. I impose the boundaries halfway between two nodes. At the left, right, and bottom boundaries there are no-slip conditions and particles are bounced back. This takes place for all Dirichlet boundary conditions except that for nonzero velocities one has to add the right momentum to the particles traveling on the diagonal links. Considering the top boundary, the population N_3 is copied into N_7 without adding an extra momentum. The population N_2 is copied into N_6 and $\frac{\overline{\rho_{LB}}}{6}u_{LB}^{top}$ is subtracted. u_{LB}^{top} is the (local) velocity at the top given by the boundary condition. A similar process occurs with the population N_4, which is converted into N_8 and $\frac{\overline{\rho_{LB}}}{6}u_{LB}^{top}$ is added.

In the case of Neumann boundary conditions, particles

traveling on diagonal links undergo a specular reflection. The required derivative at the boundary δu_{LB}^{top} is achieved by adding (or subtracting) the moment loss due to viscous stress $\frac{\overline{\rho_{LB}}}{2}\nu_{LB}\delta u_{LB}^{top} \equiv \frac{\overline{\rho_{LB}}}{2}\nu_{LB}\frac{\partial u_{LB}(x,y)}{\partial y_{LB}}\Big|_{top}$ to the reflected particles.

The use of the mean density $\overline{\rho_{LB}}$ for the calculation of the boundary conditions as well as for the calculation of N^{eq} instead of ρ_{LB} has no influence on the results within the numerical errors as long as the compressibility effect is small.

The great advantage of the LBM's is their simple and local algorithm. Only nearest neighbors are involved in the calculation, though phenomena of second order in space are described such as diffusion and Neumann boundary conditions. The algorithm consists of three substeps per time step.

(1) The boundary conditions are set according to the previous time step. The populations N_i' are calculated at the boundary. This step involves nearest neighbors.

(2) At every node new populations are calculated due to the moving of their nearest neighbors. This step involves nearest neighbors.

(3) At every node the collision term is calculated and the body forces are added. This step is completely local.

For all calculations I use the zero-speed initial condition, i.e., $N_0 \equiv d_0$ and $N_i \equiv d$.

I run the code on a DEC Alpha station for lattices up to 150 × 150 meshpoints and on a NEC SX-3-24R for larger lattices. On the DEC about 10 μs are needed per time step and node, on the NEC about 83 ns. On the NEC I achieve a performance of between 2.0 and 2.4 GFlops, which has to be related to a peak performance of 6.4 GFlops. The program has not been specially adapted for the NEC computer.

III. TEST PROBLEM

To test the LBM with the previous described boundary conditions I choose a benchmark problem originally proposed by Shih, Tan, and Hwang [6]. The geometry of the problem is a square box of 1×1 m^2 ($x_{len} = 1$ m and $y_{len} = 1$m) with no-slip boundaries conditions at the left, right, and bottom boundaries and a shear flow at the top with the velocity profile

$$u_x(x) = 16(x^4 - 2x^3 + x^2). \tag{14}$$

The maximum speed of 1 m/s is chosen as the characteristic velocity and, therefore, the Reynolds number becomes

$$\mathrm{Re} = \frac{1}{\nu}\frac{m^2}{s}. \tag{15}$$

Assuming a time-independent solution of the Navier-Stokes equations, which is true for small Reynolds numbers (Re$<$ 1000), the steady state velocity $u^\infty = (u_x^\infty, u_y^\infty)$ is set to

$$u_x^\infty = 8s(x)\,v'(y), \tag{16}$$
$$u_y^\infty = -8s'(x)\,v(y), \tag{17}$$

with $s(x) = x^4 - 2x^3 + x^2$ and $v(y) = y^4 - y^2$.

If the pressure is given by

$$p^\infty = \nu \times 8\big[S(x)v'''(y) + s'(x)v'(y)\big] + 64\big\{S_2(x)v(y)v''(y) - [v'(y)]^2\big\}, \tag{18}$$

the solution of the time-independent Navier-Stokes equations results in a body force $\vec{f} = (f_x, f_y)$,

$$f_x = 0, \tag{19}$$
$$f_y = \nu \times 8\big[24S(x) + 2s'(x)v''(y) + s'''(x)v(y)\big] + 64\big[S_2(x)V(y) - v(y)v'(y)S_1(x)\big]. \tag{20}$$

The above used functions are defined as follows:

$$S(x) = \int s(x)dx,$$
$$S_1(x) = s(x)s''(x) - [s'(x)]^2,$$
$$S_2(x) = \int s(x)s'(x)dx,$$
$$V(y) = v(y)v'''(y) - v'(y)v''(y).$$

I start with a detailed study at Re = 50 to check the influence of the density ρ_{LB}, the (characteristic) velocity u_{LB}, and the lattice size on the accuracy of the results. The difference between the theoretical and the numerical results is characterized by the relative error of the velocity and the pressure

$$\Delta u = \frac{\sqrt{\sum(u_x - u_x^\infty)^2 + (u_y - u_y^\infty)^2}}{\sqrt{\sum(u_x^\infty)^2 + (u_y^\infty)^2}} \tag{21}$$

and

$$\Delta p = \frac{\sqrt{\sum(p - p^\infty)^2}}{\sqrt{\sum(p^\infty)^2}}, \tag{22}$$

respectively. I do not find an influence of the density ρ_{LB} or the relation d_0/d on the results. In Fig. 1 the dependence of the errors for both velocity and pressure on the parameters l_y and u_{LB} are shown. The most important message of Fig. 1 is that there exists a minimum in the errors at around a certain viscosity ν_{LB}. For the pressure this viscosity is about a factor of 2 larger than for the velocity. Furthermore, there exists a lower limit for ν_{LB}. Beyond this value the solution becomes wrong. As an example, the results of a calculation for $\nu_{LB} = 2.5 \times 10^{-3}$ and $l_y = 50$ for Re = 100 are shown in Fig. 2(a). Though the error of the pressure field is rather small (see Table I), some abnormal behavior of the pressure is observed. On the contrary, the velocity field exhibits no unusual features. Using the original LBM without rest particles the origin of the vortex is shifted [see Fig. 2(b)] and the calculation loses its validity. For larger values of the vis-

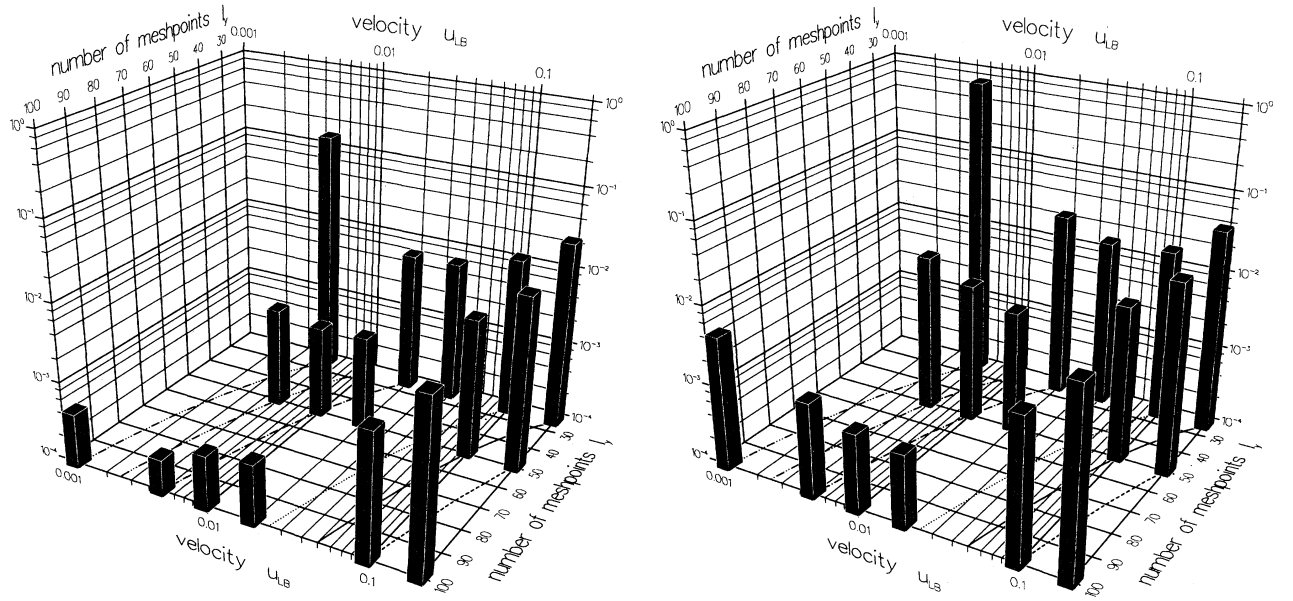

a) errors of velocity b) errors of pressure

FIG. 1. Relative errors for velocity and pressure according to the definition of Eqs. (21) and (22) for Re = 50 and different parameter configurations. The axis for the velocity u_{LB} is logarithmic for a better visualization of the results. The lines on the basic plane mark contours of constant viscosity ν_{LB}. The values for ν_{LB} are from left to right: 0.0025, 0.005, 0.01, 0.05, 0.1, and 0.2.

cosity I do not find any difference between the two kinds of methods within the numerical errors. This means that the reservoir of rest particles stabilizes the system for short relaxation times. The use of a small value for ν_{LB} is of interest for reaching high Reynolds numbers. With the lattice BGK (LBGK) method including rest particles, Hou *et al.* reach a lower limit of the viscosity of about $\nu_{LB} = 2.56 \times 10^{-3}$ [10]. For their calculations with a uniform shear velocity at the top of $u_{LB} = 0.1$ they used a 256×256 lattice for all Reynolds numbers so that for, e.g., Re = 1000, the viscosity is $\nu = 0.0256$. There is no possibility of comparing their results for the pressure

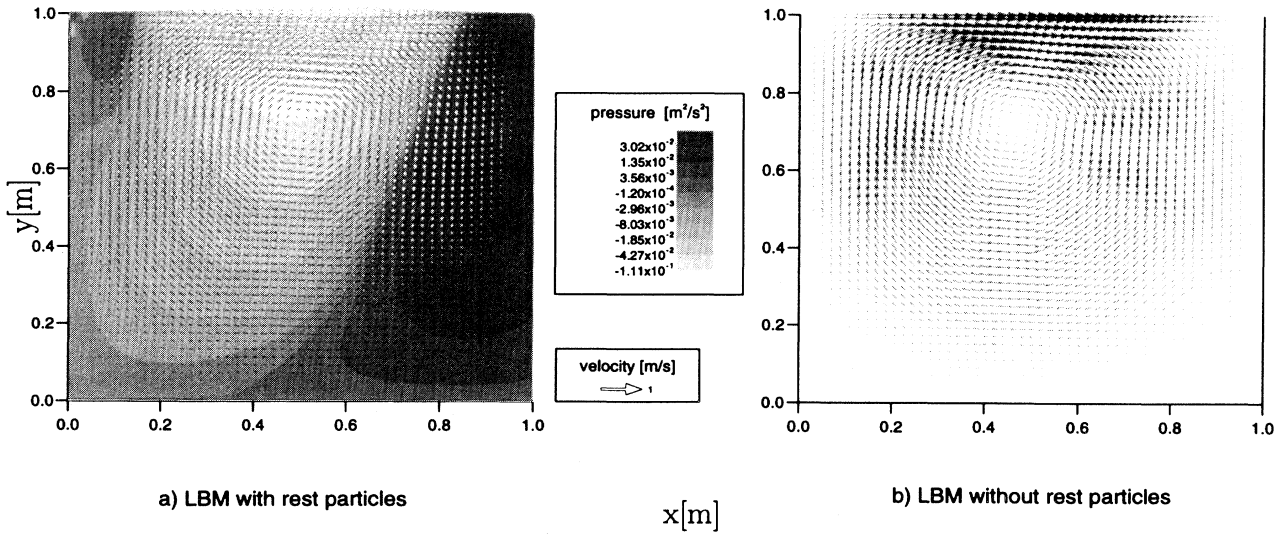

FIG. 2. Pressure and velocity profile for the test problem (Re = 100). The viscosity is $\nu_{LB} = 0.0025$.

TABLE I. Parameters and errors for the test problem with the Dirichlet boundary condition at the top. Δt is the time step of the calculation in terms of the real world. The total time indicates the time in which the system has been converged into its steady state within the numerical errors except for Re = 5000 where the calculation is extremely time consuming. The CPU time shows the consumed computer time on a DEC-Alpha station (α) or a NEC SX-3-42R (SX-3). Not all calculations for Re = 50 are listed.

Re	u_{LB}	l_y	ν_{LB}	Δt [s]	Total time [s]	CPU time [min]	Δu	Δp
10	0.04	50	0.2	8×10^{-4}	2	1 (α)	2.1×10^{-3}	5.8×10^{-3}
	0.004	50	0.02	8×10^{-5}	2	11 (α)	1.1×10^{-3}	6.8×10^{-3}
50	0.02	50	0.02	4×10^{-4}	10	11 (α)	1.7×10^{-3}	3.9×10^{-3}
	0.01	100	0.02	1×10^{-4}	10	167 (α)	4.1×10^{-4}	8.4×10^{-4}
100	0.04	50	0.02	8×10^{-4}	20	11 (α)	4.7×10^{-3}	5.0×10^{-3}
	0.005	50	0.0025	1×10^{-4}	20	84 (α)	2.8×10^{-3}	9.7×10^{-3}
	0.02	100	0.02	2×10^{-4}	20	167 (α)	1.2×10^{-3}	1.3×10^{-3}
	0.02	150	0.03	1.33×10^{-4}	20	563 (α)	7.6×10^{-4}	8.4×10^{-4}
500	0.1	100	0.02	1×10^{-3}	100	167 (α)	3.4×10^{-2}	3.3×10^{-2}
	0.04	250	0.02	1.6×10^{-4}	100	55 (SX-3)	5.4×10^{-3}	5.5×10^{-3}
1000	0.0787	254	0.02	3.098×10^{-4}	124	42 (SX-3)	2.8×10^{-2}	2.8×10^{-2}
2000	0.08	500	0.02	1.6×10^{-4}	80	167 (SX-3)	5.4×10^{-2}	5.1×10^{-2}
5000	0.05	2000	0.02	2.5×10^{-5}	12.5	2770 (SX-3)	7.7×10^{-1}	1.2×10^{0}

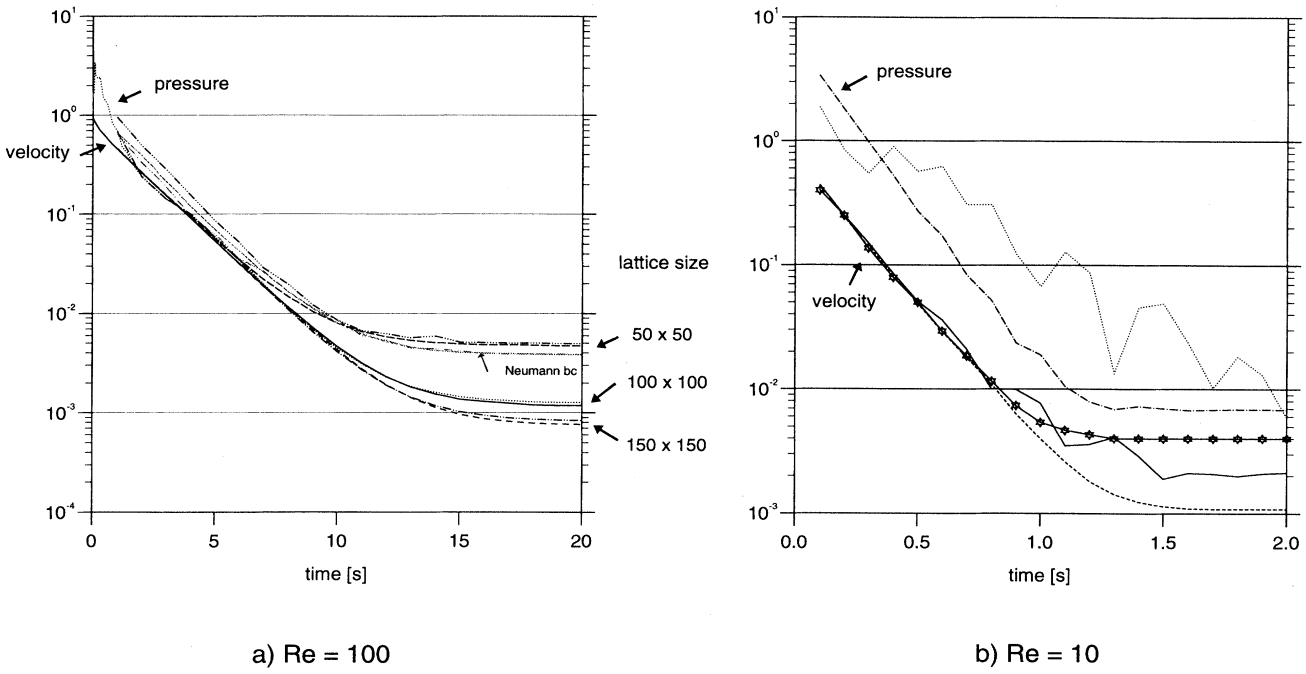

FIG. 3. Relative errors for velocity and pressure according to the definition of Eqs. (21) and (22) versus the time in the real world for Re = 100 (left) and Re=10 (right). Lines with points in its style belong to the pressure, the others to the velocity. For Re = 100 all results as listed in Table I are plotted except the case with the viscosity $\nu = 0.0025$. Also the result with the Neumann boundary condition is plotted (compare Table II). For Re = 10 the results for $u_{LB} = 0.04$ (solid line for velocity and pointed line for pressure) and $u_{LB} = 0.004$ (dashed line for velocity and dashed pointed for pressure) are shown. The line with the stars as markers is the result of a finite element calculation [11].

TABLE II. Parameters and errors for the test problem with the Neumann boundary condition at the top. Δt is the time step of the calculation in terms of the real world. The total time indicates the time in which the system has been converged into its steady state within the numerical errors. The CPU time shows the consumed computer time on a DEC-Alpha station (α) or a NEC SX-3-42R (SX-3).

Re	u_{LB}	l_y	ν_{LB}	Δt [s]	Total time [s]	CPU time [min]	Δu	Δp
50	0.02	50	0.02	4×10^{-4}	10	11 (α)	1.7×10^{-3}	2.8×10^{-3}
100	0.04	50	0.02	8×10^{-4}	20	11 (α)	3.8×10^{-3}	3.9×10^{-3}
1000	0.0787	254	0.02	3.098×10^{-4}	124	42 (SX-3)	4.5×10^{-2}	4.0×10^{-2}

with other numerical calculations, nor did they publish a comparison of the pressure field with different values for the viscosity by changing the lattice size.

The behavior of the errors in time is shown in Fig. 3 for the Reynolds numbers Re = 100 (left) and Re = 10 (right). Some oscillatory behavior of the errors is observed for Re = 10. It can be reduced by decreasing both the velocity u_{LB} and the viscosity ν_{LB} while keeping the lattice size fixed. The reason for the oscillatory behavior might be the long relaxation time (high viscosity) and the large time step (high velocity), which may result in difficulty relaxing the system into its local equilibrium in every time step. In Fig. 3(b) the errors of my calculations are compared with those of a finite element calculation with a fractional step Θ scheme where the lattice size was 64×64 [11].

I go beyond the Reynolds number of 100 and perform calculations for Re = 500, 1000, 2000, and 5000. For Re = 5000 computation becomes extremely time consuming because of the large lattice size. For smaller lattice the compressibility error becomes too large. From the calculations with the 2000×2000 mesh I observe a diminishing of the vorticity with time but it is not yet clear if the system will converge towards a steady-state-like solution with only small perturbations in time, or if the center of the main vortex will oscillate and some extra vorticities will remain. I have to stress that this case is beyond the validation capability of the analytical solution and the behavior of the system is not yet known.

Instead of applying the Dirichlet boundary condition at the top one can force the flow by the Neumann boundary condition

$$\left.\frac{\partial u_x(x,y)}{\partial y}\right|_{y=1} = 80(x^4 - 2x^3 + x^2). \tag{23}$$

I test this boundary condition for Reynolds numbers Re = 50, Re = 100, and Re = 1000. The results are listed in Table II, which shows that the Dirichlet and the Neumann boundary conditions give results of nearly the same accuracy. The convergence rate for the errors of the cal-

TABLE III. Parameters and results for the extended driven cavity problem. Re is the Reynolds number, A the aspect ratio, bc denotes the boundary condition (D: Dirichlet, N: Neumann, n: nonuniform, u: uniform), $\vec{r}$ are the coordinates of the origin of a vortex.

ν	Re	A	bc	mesh size	ν_{LB}	$\vec{r}$ of 1.vortex	$\vec{r}$ of 2.vortex
0.10	10	10	D,u	500×50	0.05	(9.15, 0.63) m	
0.02	50	1.0	D,n	100×100	0.02	(0.56, 0.76) m	
0.02	50	10	D,n	1000×100	0.02		
0.02	50	50	D,n	10000×100	0.02		
0.02	29	1.0	N,n	100×100	0.02	(0.57, 0.78) m	
0.02	57	10	N,n	1000×100	0.02		
0.001	295	1.0	D,n	254×254	0.02	(0.60, 0.64) m	
0.001	580	10	D,n	2540×254	0.02	(8.07, 0.55) m	
0.001	1000	1.0	D,n	254×254	0.02	(0.54, 0.57) m	
0.001	1000	10	D,n	2540×254	0.02	(8.34, 0.52) m	
0.001	1000	50	D,n	25400×254	0.02		
0.001	1016	1	D,u	254×254	0.02	(0.53, 0.56) m	
0.001	1016	10	D,u	2540×254	0.02	(9.16, 0.57) m	(7.83, 0.59) m
0.001	295	1.0	N,n	254×254	0.02	(0.60, 0.64) m	
0.001	580	10	N,n	2540×254	0.02	(9.16, 0.54) m	(7.59, 0.63) m
0.001	830	10	N,n	2540×254	0.02	(9.35, 0.55) m	(7.81, 0.77) m
0.001	880	50	N,n	25400×254	0.02		
0.001	630	10	N,u	2500×250	0.02	(9.34, 0.56) m	(7.57, 0.63) m

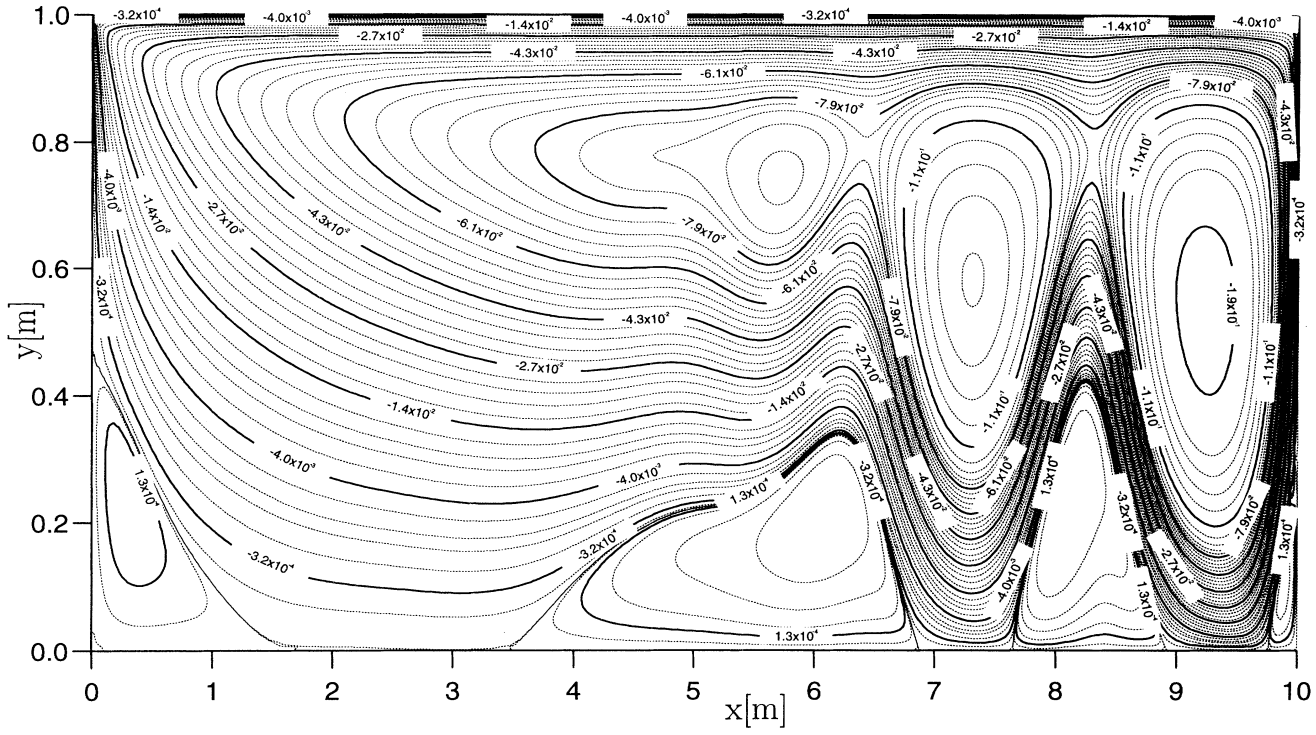

FIG. 4. Streamlines for Re = 1000, aspect ratio $A = 10$, and the uniform Dirichlet boundary condition at the top.

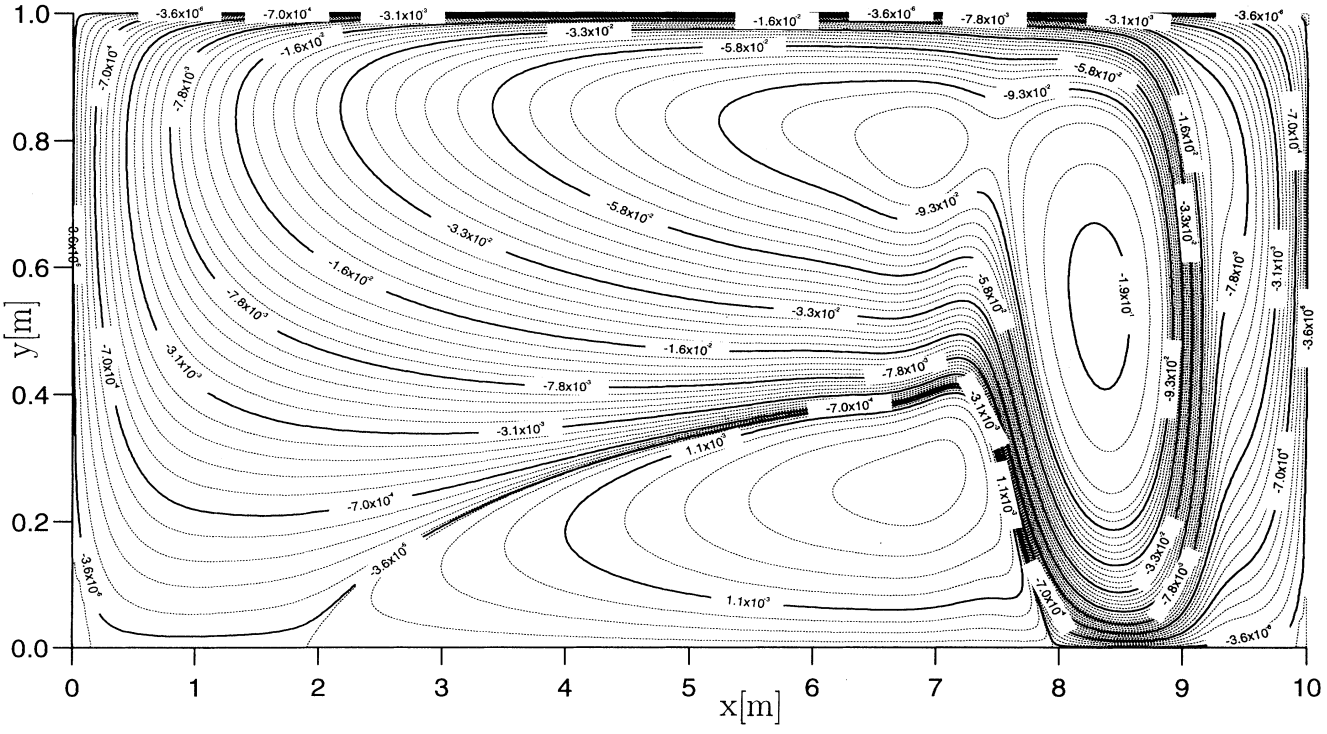

FIG. 5. Streamlines for Re = 1000, aspect ratio $A = 10$, and the nonuniform Dirichlet boundary condition at the top.

culation for Re = 100 can be seen in Fig. 3(a). It is of the same order as for the Dirichlet boundary condition.

IV. EXTENDED DRIVEN CAVITY PROBLEM

In the preceding section I have verified that the LBM with enhanced collisions and rest particles reproduces the flow in a lid-driven cavity very nicely. Now I study the flow in a cavity with four different types of boundary conditions (uniform and nonuniform Dirichlet, uniform and nonuniform Neumann) and perform runs for different aspect ratios $A := \frac{x_{len}}{y_{len}}$ $(A = 1, 10, 50)$. The calculations are listed in Table III. The shear flow at the top for the nonuniform cases is defined in the same manner as in the test case. Explicitly, they are given as follows: the y axis is fixed to length 1 for all calculations ($y_{len} = 1\text{m}$). Defining a new variable $\tilde{x} = A^{-1}x$, with $0 \leq \tilde{x} \leq 1$, the Dirichlet boundary condition is written as

$$u_x(x, 1) = 16(\tilde{x}^4 - 2\tilde{x}^3 + \tilde{x}^2) \tag{24}$$

and the Neumann boundary condition as

$$\left.\frac{\partial u_x(x,y)}{\partial y}\right|_{y=1} = 80(\tilde{x}^4 - 2\tilde{x}^3 + \tilde{x}^2). \tag{25}$$

The difference between nonuniform and uniform shear flow is the strong curvature of the streamlines in the corners of the latter. This fact has only a marginal influence on the main stream if the aspect ratio is $A = 1$ (see Table III), but for an aspect ratio of $A = 10$ the strong curvature causes a small vortex on the right-hand side even for Re = 10. In the case of the nonuniform shear flow and a small Reynolds number (Re = 50) the streamlines are stretched with increasing aspect ratio and the inflection line between forward and back flow lies very near the theoretical value ($y = 2/3\, y_{len}$) for an infinitely long cavity with a constant flow (constant top velocity).

For the Reynolds number Re = 1000 a different behavior of the flow is observed for $A = 10$. By applying a uniform shear flow at the top two strong vortices are formed on the right-hand side (Fig. 4). The case with the nonuniform shear flow exhibits only one strong vortex (Fig. 5), because a high pressure zone at the end of the cavity is built up (see Fig. 6).

The difference between the Dirichlet and the Neumann boundary conditions is best seen from the velocity profile at the top, which is shown in Fig. 7 for three different Reynolds numbers for the nonuniform case and one

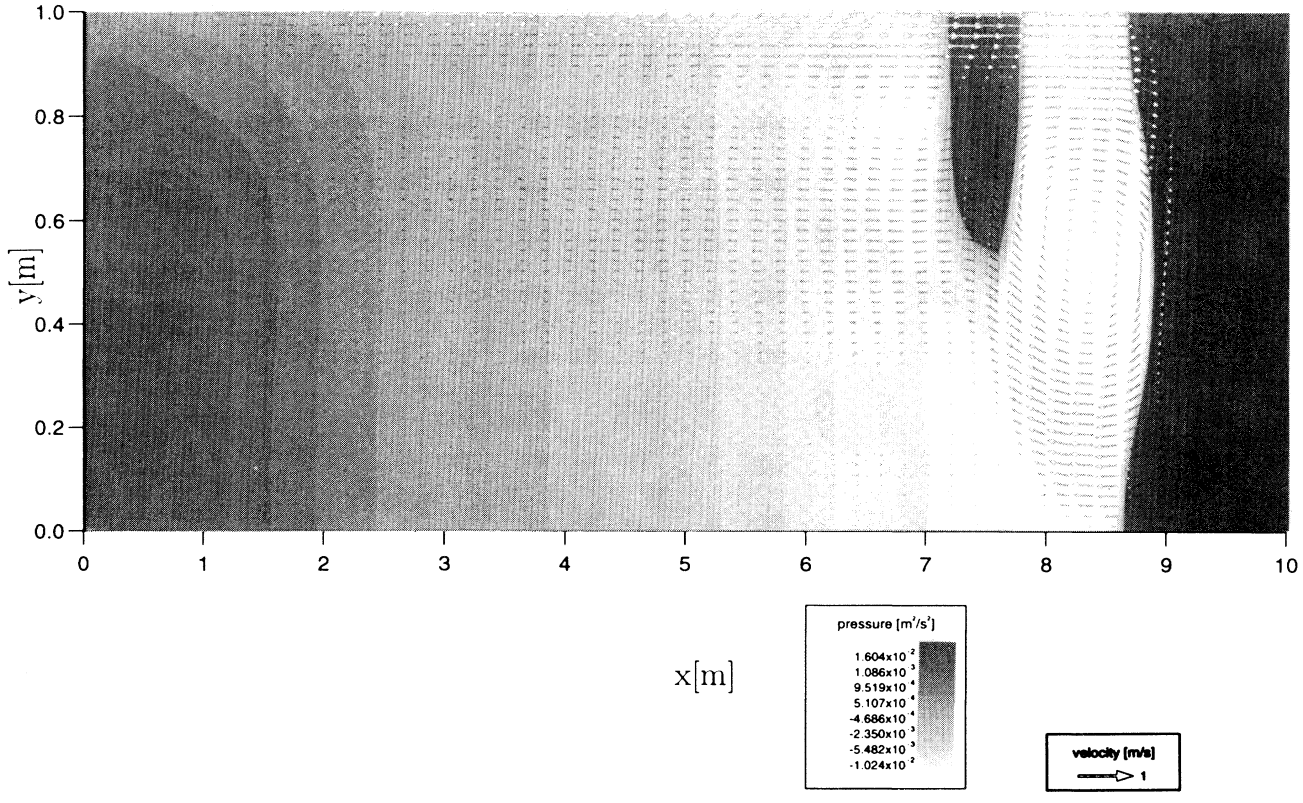

FIG. 6. Pressure and velocity profile for Re = 1000, aspect ratio $A = 10$, and the nonuniform Dirichlet boundary condition at the top.

Reynolds number for the uniform case. The main difference between the uniform and nonuniform boundary conditions is the more pronounced second vortex for the uniform case (compare Fig. 8 and Fig. 9). It would be of interest to go beyond an aspect ratio of $A = 10$, but since the lattice Boltzmann model at the present stage needs a uniform mesh, the calculations will consume a lot of computer time. For this purpose a new model is under development which allows one to use a regular but nonuniform mesh. Therefore, only two runs for the nonuniform shear flow at the top has been performed, showing that the vortex on the right-hand side disappears completely.

V. CONCLUSION

In this paper I have shown that the lattice Boltzmann method with enhanced collisions and rest particles is a fast and accurate method for calculating the velocity and the pressure in a driven cavity by comparing the numerical results with the analytical solution of the problem. Using the Dirichlet or the Neumann boundary condition for the forced flow at the top makes no difference in the convergence behavior of the numerical results. This is a very striking observation because the implementation of the Neumann boundary condition in the LBM is extremely easy and involves only nearest neighbors. It is possible to decrease the viscosity beyond the value $\nu_{LB} = 0.014$, which was found to be the lower limit for the LBM without rest particles. The pressure is more sensitive to relaxation problems than the velocity.

In the second part of this paper I have presented the results for a driven cavity problem with a uniform or nonuniform shear flow at the top and aspect ratios greater than one. The results of the calculations with the Dirichlet boundary condition are compared with those of the

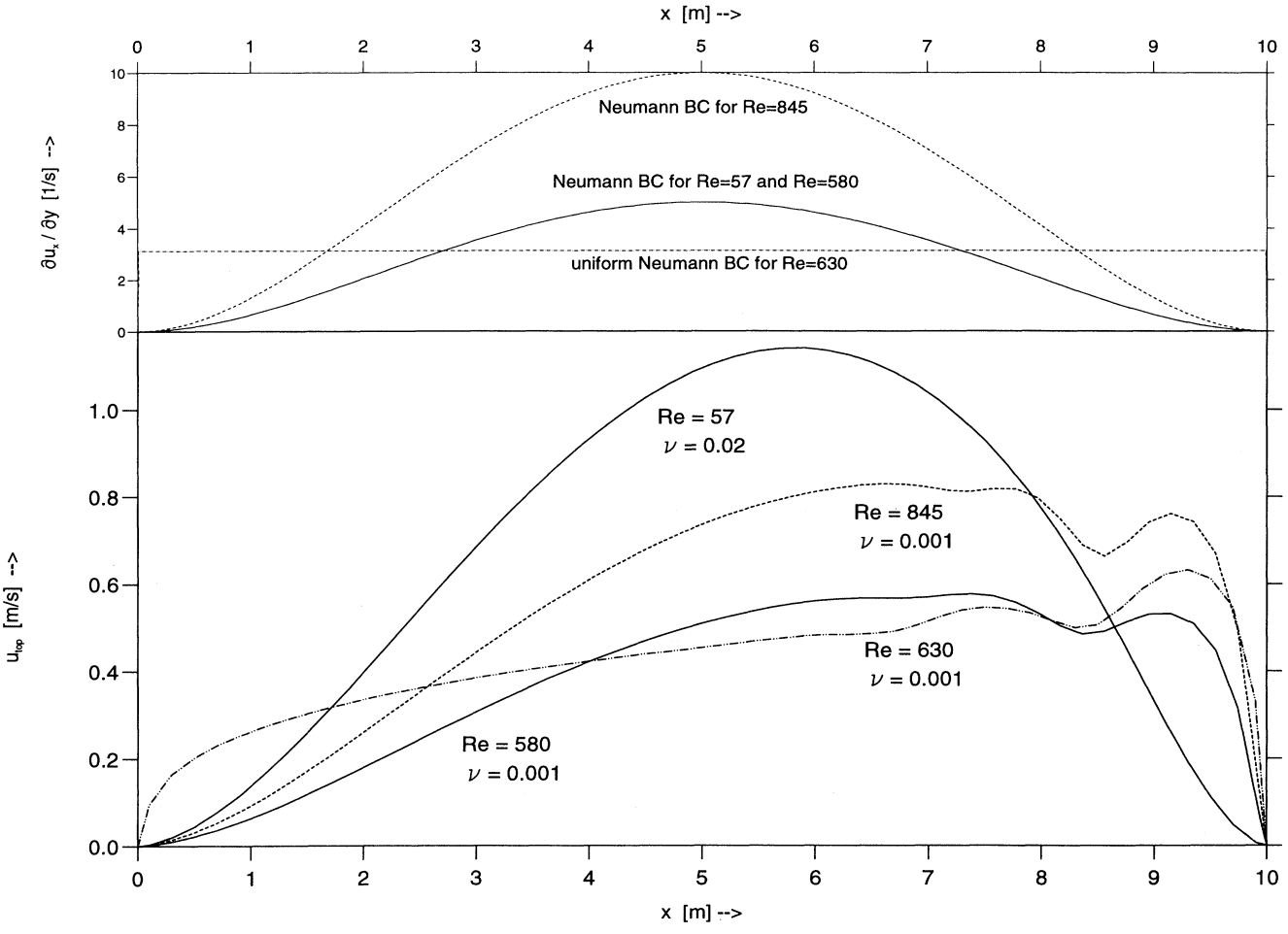

FIG. 7. Velocity at the top for different Reynolds numbers when the Neumann boundary condition is applied at the top. The aspect ratio is $A = 10$, the viscosity $\nu = 0.001$ m^2/s for the high Reynolds numbers, and $\nu = 0.02$ m^2/s for the low Reynolds number. The point-dashed lines correspond to the uniform Neumann boundary condition (Re = 630).

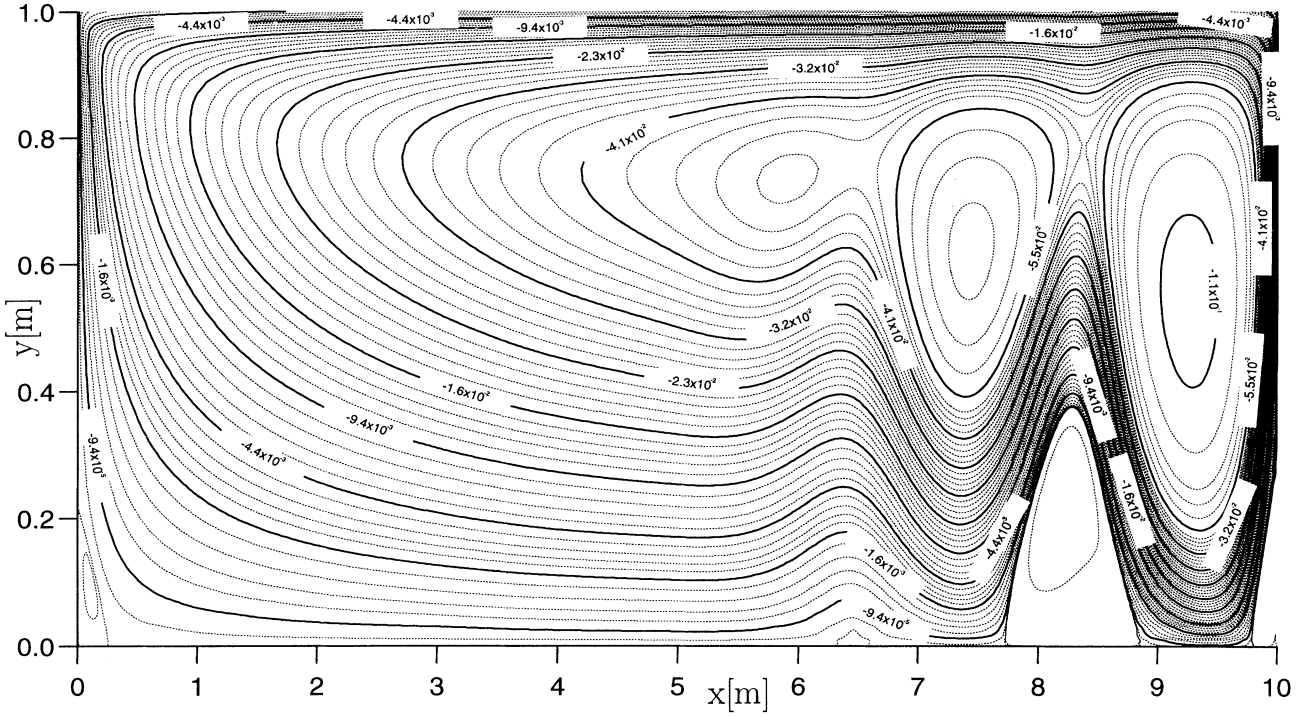

FIG. 8. Streamlines for Re = 630, aspect ratio $A = 10$, and the uniform Neumann boundary condition at the top.

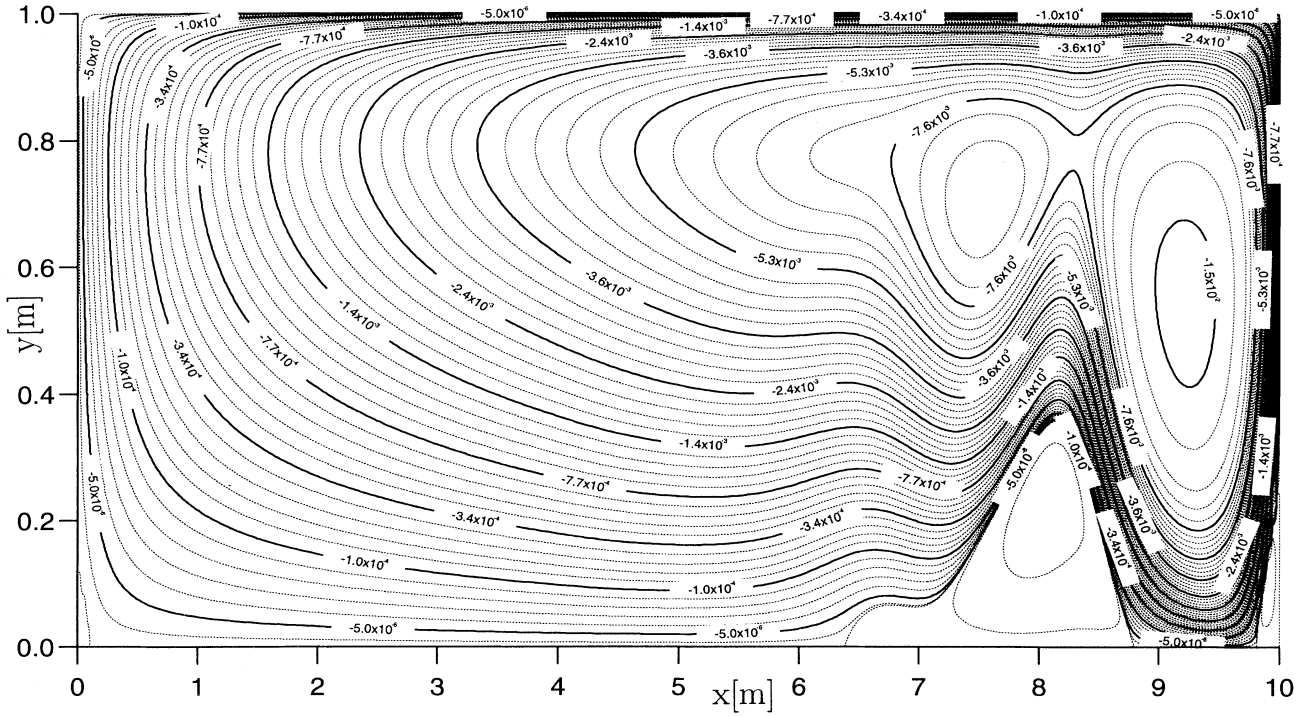

FIG. 9. Streamlines for Re = 580, aspect ratio $A = 10$, and the nonuniform Neumann boundary condition at the top.

Neumann boundary condition. For an aspect ratio of $A = 1$ the type of boundary condition has only a small influence on the vortex structure. For an aspect ratio of $A = 10$ significant differences have been found for the various boundary conditions. A further improvement of the lattice Boltzmann model would make it possible to perform runs with very large aspect ratios, which appear in the problem of the flow in shallow water.

ACKNOWLEDGMENTS

I would like to thank G. Zanetti and R. Benzi for many fruitful discussions. I am much indebted for the high amount of computer time on the NEC SX3-42R supercomputer offered by the CSCS in Manno (Switzerland). This work has been carried out with the financial contribution of Sardinia Regional Authorities.

[1] U. Frisch, B. Hasslacher, and Y. Pomeau, Phys. Rev. Lett. **56**, 1505 (1986).
[2] G. McNamara and G. Zanetti, Phys. Rev. Lett. **61**, 2332 (1988).
[3] F. Higuera, S. Succi, and R. Benzi, Europhys. Lett. **9**, 663 (1989).
[4] Y.H. Qian, D. D'Humières, and P. Lallemand, Europhys. Lett. **17**, 479 (1992).
[5] H. Chen, S. Chen, and W.H. Matthaeus, Phys. Rev. A **45**, R5339 (1992).
[6] T.M. Shih, C.H. Tan, and B.C. Hwang, Int. J. Numer. Methods Fluids **9**, 193 (1989).
[7] D. D'Humières, P. Lallemand, and U. Frisch, Europhys. Lett. **2**, 291 (1986).
[8] R. Benzi, S. Succi, and M. Vergassola, Phys. Rep. **222**, 146 (1992).
[9] S. Succi (private communication).
[10] S. Hou, Q. Zou, S. Chen, G.D. Doolen, and A.C. Cogley (unpublished).
[11] Petr Klouček and Franz S. Rys, SIAM J. Numer. Anal. **31**, 1312 (1994).

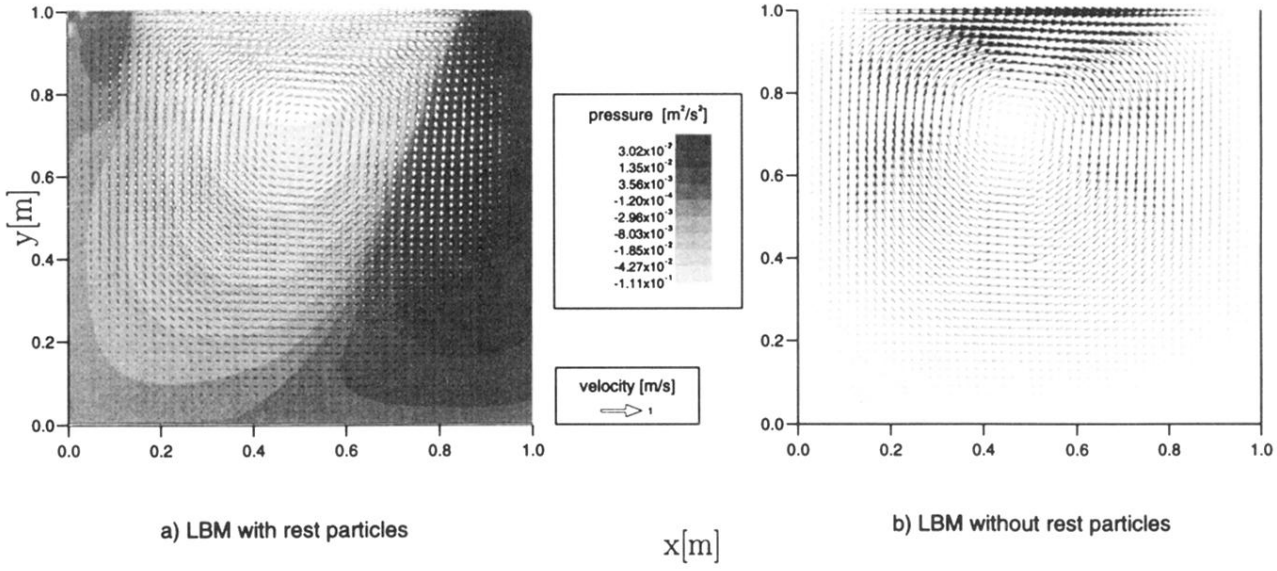

FIG. 2. Pressure and velocity profile for the test problem (Re = 100). The viscosity is $\nu_{LB} = 0.0025$.

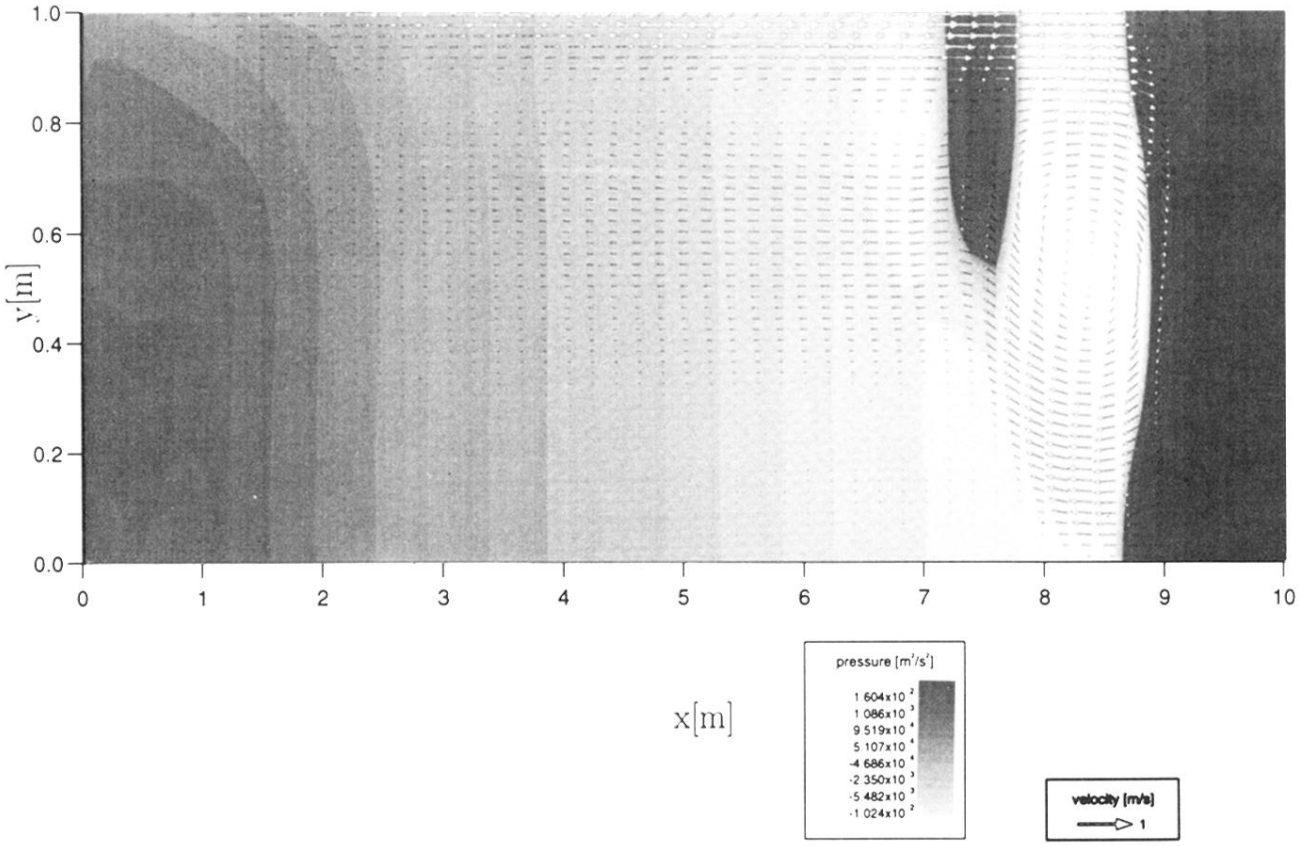

FIG. 6. Pressure and velocity profile for Re = 1000, aspect ratio $A = 10$, and the nonuniform Dirichlet boundary condition at the top.